Available online at www.sciencedirect.com

ScienceDirect

Physics Procedia 3 (2010) 225–233

Physics Procedia

www.elsevier.com/locate/procedia

International Congress on Ultrasonics, Universidad de Santiago de Chile, January 2009

A comparative study of four vector velocity estimation methods applied to flow imaging

Adrien Marion*, Walid Aoudi, Adrian Basarab, Philippe Delachartre, Didier Vray

University of Lyon, Creatis-Lrmn; CNRS UMR 5220; INSERM U630;
University Lyon 1; INSA-Lyon, 7 Avenue Jean Capelle, 69621 Villeurbanne Cedex, France

Abstract

Ultrasonic imaging is often used to estimate blood flow velocity. Estimates are currently performed by Doppler-based techniques but they suffer from some shortcomings. This article compares four vector velocity estimation methods complementary to Doppler. Each method has been applied to six sequences, simulated and experimental, with various flow parameters. Results are presented in several curves and show specificities of each method.

Keywords: blood flow; decorrelation; spatiotemporal filtering; speckle tracking; ultrasound imaging; vector velocity

* Corresponding author. Tel.: (+33) 4 72 43 87 86 ; fax: (+33) 4 72 43 85 26.
E-mail address: adrien.marion@creatis.insa-lyon.fr

doi:10.1016/j.phpro.2010.01.031

1. Introduction

Blood velocity estimation is required in many clinical applications. Ultrasonic imaging is often used to reach this goal because of its ability to provide images in real-time. Currently, for clinical diagnosis, velocity estimates are performed by Doppler-based techniques. Results are displayed at a frame rate close to B-mode images acquisition rate. Several techniques using the Doppler effect have been proposed. Notably, Kasai [1] has developed a real-time autocorrelation estimator that evaluates the average phase shift related to the axial velocity. However, Doppler techniques suffer from a number of limitations:

- low velocities are inadequately estimated
- and the spatial resolution of the results is limited

Moreover, only the axial component of the velocity is estimated. Consequently,

- the flow orientation must be known to estimate the velocity modulus
- and the angle between the flow and the probe into the imaging plane must be smaller than 60°.

New methods have been proposed to overcome these shortcomings. Ferrara and Algazi [2] proposed a maximum likelihood estimator for velocity from a stochastic model of the signal from a point scatterer. It exploits the effect of the scatterer velocity on both the time delay and the shift in frequency. In order to estimate vector velocity instead of the only axial component, original approaches have been developed. The most known is the speckle tracking presented by Bohs et al. [3]. It is based on the maximization of a similarity measure between two blocks from two successive images. Basarab et al. proposed an evolution of this approach based on a bilinear deformable model. This model is then well adapted to blood flow evaluation since it estimates subpixelic displacements [4-5]. Jensen et al. [6] suggested using directional beamforming to estimate both magnitude and orientation of the flow. Other methods exploit the statistics of ultrasonic images [7-8]. They associate targets velocity to signal decorrelation. Recently, Marion et al. [9-10] presented a velocity estimator based on a bank of spatiotemporal oriented filters. Besides, Oddershede et al. [11] proposed two estimators based on the search of the plane in the 3D Fourier space where energy is essentially concentrated.

In this article, we propose to compare four vector velocity estimation methods [3,5,8,9] applied to flow imaging. We are particularly interested in cases where Doppler techniques are inefficient. Thus, we will study cases with flow angles between 60° and 90° (longitudinal flow). This comparison is performed on experimental and simulated data. In section B.1, we recall the principles of the several methods. In section B.2, we give details about the data used. The results are presented in section C then discussed in section D. Finally, we conclude about advantages and drawbacks of each method.

2. Methods and material

2.1. Blood flow estimation methods

The goal of this study is to provide quantitative results about performances of the estimates performed with different methods for various flow cases. The different methods compared in this paper are:

- block matching (BM) [3]
- bilinear deformable block matching (BDBM) [5]
- speckle flow index (SFI) [8]
- spatiotemporal filtering (STF) [9]

These four methods are rapidly presented in the next four sections.

2.1.1. Block matching

The method presented in [3] is a block-matching method. It is called speckle tracking in ultrasound imaging. The principle of the method is to find the better block in image 2 compared to a reference block defined in image 1. The better block is found by an algorithm that minimizes a similarity criterion. Several cost functions can be implemented, for examples: the sum of square distances (SSD), the normalized cross correlation (NCC) or the sum of absolute distances (SAD) which is used for this study. The factor of interpolation is set to 9.

2.1.2. Bilinear deformable block matching

The method presented in [5] uses a parametrical motion model for controlling the local deformations. Thus, in contrast to classical BM method, this method employs a bilinear model with eight parameters instead of pure translations. With BDBM method, a collection of nodes is placed on top of the reference image. The bilinear parameters are estimated in rectangular regions of interest taken around each node. This is achieved using an iterative approach. Note that with this method the size of the ROIs is considered larger than the mesh step, which involves an overlapping between neighbouring regions of interest. This overlapping is taken into account when computing the dense displacement field. The factor of interpolation is set to 9.

2.1.3. Speckle flow index

The method presented in [8] is based on a spatiotemporal analysis of the changes of the speckle pattern. The amount of change in the morphology of the speckle along time is directly related to the second order statistics. The decorrelation law during time of the speckle in a fluid depends on the flow velocity, on the point spread function of the imaging system (PSF) and on the framerate. The principle of the SFI method consists in the estimation of the normalized local temporal variance of one pixel across the direction z directly from image sequences. It takes into account the specificity of the images (emitting frequency, spatial resolution, flow range, temporal sampling rate).

2.1.4. Spatiotemporal filtering

The method presented in [9] is based on a spatiotemporal approach. A sequence in translation leaves a trace of speckle in the 2D+t volume of data. Thus, motion is related to texture orientation in the spatiotemporal domain. Each pixel of the sequence has a different velocity and consequently the orientation is local. The authors estimate orientations locally by using a bank of 3D oriented filters then deduce dense fields of velocities. Note that this method performs estimates with a temporal neighbouring of around ten frames whereas block-matching methods use only two frames.

2.2. Material

The four methods presented in the previous section have been applied to six flow sequences with different velocities and orientation. Four sequences were simulated by a system approach with a 3D set of moving scatterers. Two sequences were realized by injecting blood mimicking fluid in a wall-less calibrated flow phantom. The two following sections give details about these data.

2.2.1. Simulated sequences

Blood flow sequences have been simulated in order to compare the methods. The simulation was based on the system approach of Meunier & Bertrand [12]. In order to have a realistic simulation, a 3D set of scatterers have been generated then displaced following a paraboloid law. The diameter of the vessel was equal to 1mm. An out-of-plane angle equal to 5° was used for the simulation in order to be closer to real situations. The convolution was performed by using a numerical convolution algorithm after approximation of the scatterers to nodes of a sampled grid. RF

images were demodulated then log-compressed to create sequences of B-mode images at 30 frames per second. Central frequency was set to 40MHz. Axial and lateral resolutions are respectively equal to 40µm and 80µm.

Let us define θ the angle between the probe and the vessel into the imaging plane and $\overline{v}$ the mean velocity. The four simulated sequences are:

S1 with θ=90° and $\overline{v}=0.4mm/s$
S2 with θ=80° and $\overline{v}=0.4mm/s$
S3 with θ=70° and $\overline{v}=0.8mm/s$
S4 with θ=60° and $\overline{v}=0.8mm/s$

2.2.2. Experimental sequences

A phantom in gelatin was used to simulate biological tissues. Silica was added to the composition of the phantom to replace scatterers. A blood vessel (diameter < 1mm) was constructed inside the phantom. Blood-mimicking fluid (BMF) [13] was injected into the vessel using a motor-controlled pump (Pump 11, Harvard Apparatus). The mean velocity was smaller than 1mm/s. The fluid consists of 5µm diameter nylon scattering particles (Orgasol, ELF, Atochem, Paris, France). It has been shown that the characteristics of BMF are close to those of human blood.

An ultrasonic system (Vevo 660, Visualsonics, Toronto) operating at 40MHz was used to acquire sequences of 300 B-mode images at 30 frames per second. Axial and lateral resolutions are respectively equal to 40µm and 80µm.

The two experimental sequences are:

S5 with θ=90° and $\overline{v}=0.5mm/s$
S6 with θ=80° and $\overline{v}=0.53mm/s$

3. Results

3.1. Performance criteria

Each of the four methods (BM, BDBM, SFI and STF) has been applied to the six sequences. Each method provided for each sequence a dense field of velocities into a ROI. We selected 15 velocity profiles for a given column along the time. Then, we computed means and standard deviations along the 15 temporal estimates. Thus, each method provides for each sequence two vectors containing means and standard deviations corresponding to a velocity profile inside the vessel.

We define several performance criteria to quantify the accuracy of estimates with each of the methods. The first one is the computation time T. We define two criteria E_x and E_y as the normalized mean error on v_x and v_y. Fig. 1 represents the vector velocity components v_x and v_y within the frame of reference (x,y,z). The general expression of the mean error is given in Eq. (1):

$$\overline{E} = \frac{1}{N}\sum_{i=1}^{N}\left|\frac{\hat{v}_i - v_i}{v_{mean}}\right| \qquad (1)$$

with $\hat{v}_i$ the estimated velocity at depth i, v_i the theoretical value according to the parabolic profile and v_{mean} the mean velocity of the flow.

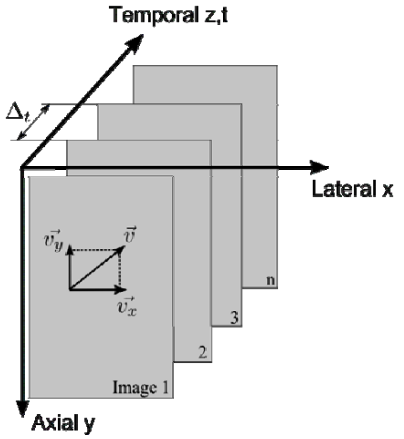

Fig.1 Definition of the vector velocity components within the schematic frame of reference (x,y,z)

Two others measures are the normalized mean standard deviations $\overline{std_x}$ and $\overline{std_y}$ on v_x and v_y whose the general expression is expressed in Eq. (2):

$$\overline{std} = \frac{1}{N}\sum_{i=1}^{N}\left(\frac{\widehat{std}_i}{v_{mean}}\right) \tag{2}$$

where $\widehat{std}_i$ is the standard deviation calculated at depth i.

We also calculate $\overline{v_x}$ and $\overline{v_y}$, the estimated mean velocities inside the vessel. Then the four last criteria are the mean modulus $\overline{|v|}$, defined in Eq. (3):

$$\overline{|v|} = \frac{1}{15}\sum_{i=1}^{15}\sqrt{\overline{v}_{x_i}^{\,2} + \overline{v}_{y_i}^{\,2}} \tag{3}$$

with the associated mean standard deviation $std_{|v|}$ and the mean orientation $\overline{\theta}$, defined in Eq. (4):

$$\overline{\theta} = \frac{1}{15}\sum_{i=1}^{15} arc\tan\left(\frac{\overline{v}_{y_i}^{\,2}}{\overline{v}_{x_i}^{\,2}}\right) \tag{4}$$

with the associated mean standard deviation.

3.2. Quantitative results

The values of the performance criteria have been calculated for each method applied to each sequence. Note that the values of $\overline{E_y}$ and $\overline{std_y}$ for S1 and S5 are not in percent because normalization is impossible. Fig.2 displays four velocity profiles estimated with each method for S1. In this case, the flow is longitudinal and consequently the modulus is approximately equal (neglecting the slight out-of-plane angle equal to 5°) to the component v_x. We also

constructed several curves. For each figure, the theoretical values are represented with black points, BM method with plus, BDBM method with circles, SFI method with squares and STF method with diamonds. SFI performs only the vector velocity modulus and so is not represented in each figure.

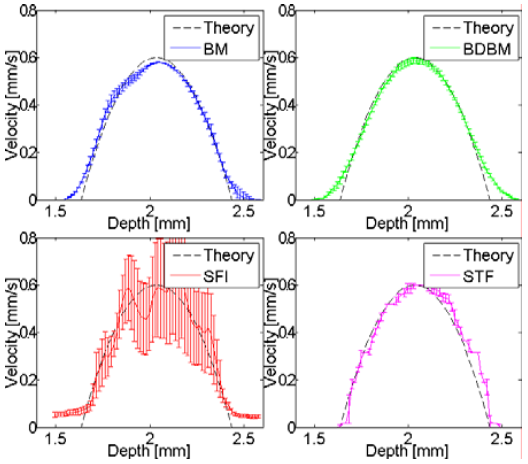

Fig.2 Velocity profiles estimated with each method for S1.

Fig.3 displays the values of the normalized mean error $\overline{E_x}$ for each method applied to each sequence.
Fig.4 displays the values of the normalized mean error $\overline{E_y}$ for each method applied to each sequence.
Fig.5 displays the values of the mean velocity v_x for each method applied to each sequence.
Fig.6 displays the values of the mean velocity v_y for each method applied to each sequence.

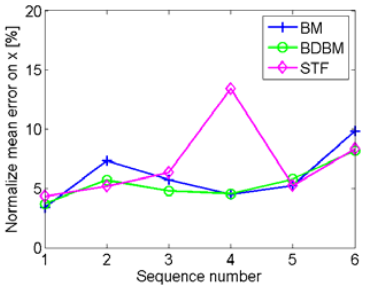

Fig.3 Normalized mean error $\overline{E_x}$ for each method applied to each sequence.

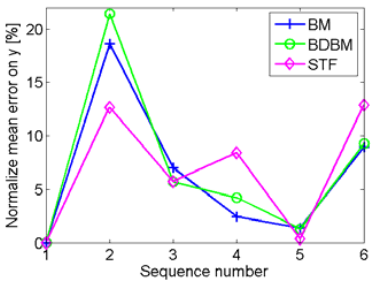

Fig.4 Normalized mean error $\overline{E_y}$ for each method applied to each sequence.

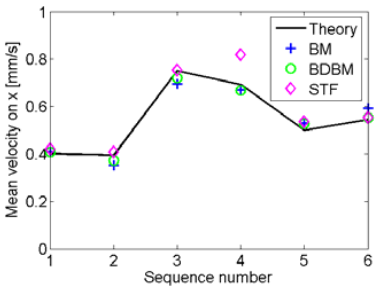

Fig.5 Mean velocity $\overline{v_x}$ for each method applied to each sequence.

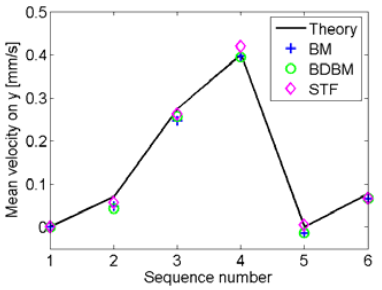

Fig.6 Mean velocity $\overline{v_y}$ for each method applied to each sequence.

Fig.7 displays the values of the mean velocity modulus $\overline{|v|}$ for each method applied to each sequence.
Fig.8 displays the values of the mean orientation $\overline{\theta}$ for each method applied to each sequence.

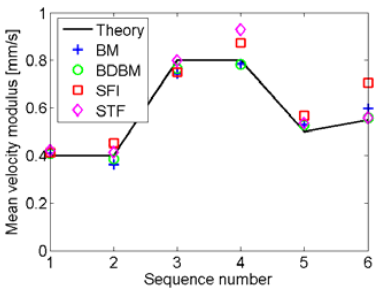

Fig.7 Mean velocity modulus $\overline{|v|}$ for each method applied to each sequence.

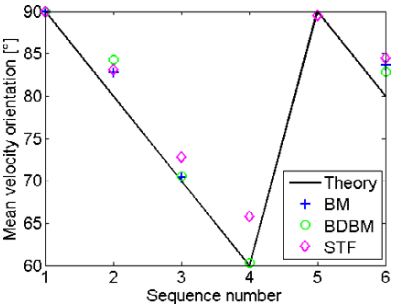

Fig.8 Mean velocity orientation $\overline{\theta}$ for each method applied to each sequence.

4. Discussion

We applied four velocity estimation methods on six sequences, experimental and simulated, with flow angles within the imaging plane from 60° to 90°. SFI estimates the 3D modulus of the vector velocity whereas BM, BDBM and STF estimate the two components of the velocity within the imaging plane. Thus, they do not give the same information about the flow.

BM performs accurate estimates on v_x; The mean error $\overline{E_x}$ is less than 10% for each sequence with a mean standard deviation $\overline{std_x}$ less than 9%. However, estimation errors on v_y are globally more important with higher values of $\overline{std_y}$. BM seems to be not sensitive to orientation. BDBM provides estimates with accuracy close to those obtained with BM. $\overline{E_x}$ is less than 9% with $\overline{std_x}$ less than 12%. Like with BM, estimates on v_y are less accurate with BDBM. Moreover, like BM, BDBM is not sensitive to orientation. STF performs good estimates; except for S4, $\overline{E_x}$ is less than 9% with $\overline{std_x}$ less than 5%. In the same way, the mean error and the mean standard deviation on v_y are higher. Contrary to BM and BDBM, STF seems to be sensitive to orientation.

Mean velocity components v_x and v_y have been estimated with BM, BDBM and STF. Estimated mean velocities with BM and BDBM are very similar. They are globally underestimated but close to theoretical values.

Estimates of mean velocity components are slightly better with STF except for S4. Note that the null velocity component v_y is perfectly estimated with all the methods for S1 and not exactly for S5.

As we could predict, estimated modulus with BM and BDBM are close and globally less than theoretical values. Nevertheless, BDBM is slightly better than BM. Except for S4, STF gives estimates for modulus globally better than those obtained with BM and BDBM. SFI estimates modulus with an accuracy slightly less interesting. However, SFI gives us estimates for a ROI of 80*40 pixels in 6.7ms whereas other methods require a few tens of seconds, respectively 17s, 39s and 40s with STF, BDBM and BM. These computation time have been estimated with Matlab 7.2 on a core 2 duo processor (2.66GHz) with 3Gb of RAM. Moreover, estimates performed by SFI are related to the 3D velocity modulus contrary to BM, BDBM and STF that performs the apparent vector velocity within the imaging plane. Thus, when the out-of-plane angle becomes important (more than 30°), SFI is the only method capable to estimate reliable velocities.

Orientation is better estimated with the region-based approaches, BM and BDBM, in comparison to the spatiotemporal approach, STF. Indeed, STF often underestimates orientation. BM and BDBM estimate orientation with a great accuracy, especially when it increases.

To conclude about these observations, we can say that:

- SFI is well adapted to out-of-plane flow contrary to the three other methods
- SFI is the only real-time method to estimate velocity
- BM, BDBM and STF gives results with similar accuracy
- STF is more sensitive to large orientation than BM and BDBM
- STF is well adapted to low orientation whereas BM and BDBM are well adapted to large orientation
- BM and BDBM are more robust in terms of velocity range. By using the tangent function, STF is limited to displacements less than 8 pixels/frame before saturating
- Estimates with BM and BDBM are very similar in terms of errors and standard deviations. This can be explained by the sequences studied here. Displacements between two images are less than 3 pixels and consequently the motion is quasi rigid. It has been verified thanks to complementary experiences that the increase of the velocity, from 0.8mm/s to 2mm/s for example, give an advantage to BDBM that is more adapted to complex motion.

5. Conclusion

In this paper, we compared four velocity estimation methods applied to flow imaging. We selected three kinds of methods: two region-based approaches, block matching (BM) and bilinear deformable block matching (BDBM), one decorrelation-based approach, speckle flow index (SFI), and one spatiotemporal approach, spatiotemporal filtering (STF). We applied theses methods on six flow sequences with orientation between the probe and the flow within the imaging plane from 60° to 90°. Four sequences were simulated with a convolution-based method. The model used a 3D set of moving scatterers to be as realistic as possible. Two experimental sequences were realized with a gelatine phantom and a blood-mimicking fluid.

We show that SFI is capable to estimate the 3D modulus of the flow velocity whereas STF, BM and BDBM estimate the two components within the imaging plane. Consequently, SFI can provide velocity information even if the out-of-plane angle of the flow is close to 90°. Furthermore, SFI is a real-time method contrary to other ones. However, SFI is less accurate than BM, BDBM and STF that are more or less equivalent. Standard deviations are clearly superior with SFI and estimated moduli are less precise. We also show that estimates performed with BM and BDBM are very similar. This can be explained by the situations studied in this paper that presents low displacements. Then, the motion is quasi rigid and so BM, which is less adapted to complex motion than BDBM, is not penalized. An increase of the displacements would add shear components taken into account by BDBM. STF gives interesting results in comparison to region-based methods. Except for a sequence with the larger orientation, criteria used in the paper show good performances with STF. It is particularly interesting because spatiotemporal methods have not been explored a lot for flow evaluation.

Acknowledgements

This work was supported by the French Ministry of higher education and research. The authors wish to thank S. Foster and A. Needles from Sunnybrook Health and Sciences Centre, Toronto, Canada, where the experiments were conducted.

References

[1] C. Kasai, N. Namekawa, A. Koyano and R. Omoto, "Real-time two-dimensional blood flow imaging using an autocorrelation technique," IEEE Trans. Son. Ultras., vol. 32, pp. 458-463, 1985.
[2] K.W. Ferrara and V.R. Algazi, "A new wideband spread target maximum likelihood estimator for blood velocity estimation-Part 1: Theory," IEEE Trans. Ultras., Ferro., Freq. Contr., vol. 38, pp. 1-16, 1991.
[3] L.N. Bohs, B.J. Geiman, M.E. Anderson, S.C. Gebhart and G.E. Trahey, "Speckle tracking for multidimensional flow estimation," Ultrason., vol. 38, pp. 369-375, 2000.
[4] A. Basarab, W. Aoudi, H. Liebgott, D. Vray and P. Delachartre, "Parametric deformable block matching for ultrasound imaging," Proc. of IEEE ICIP, vol. 2, pp. 429-432, 2007.
[5] A. Basarab, H. Liebgott, F. Morestin, A. Lyshchik, T. Igashi, R. Asato and P. Delachartre, "A method for vector displacement estimation with ultrasound imaging and its application for thyroid nodular disease," Med. Ima. Ana., vol. 12, pp. 259-274, 2007.
[6] J.A. Jensen, N. Oddershede, "Estimation of velocity vectors in synthetic aperture ultrasound imaging, " IEEE Trans. Med. Ima., vol 25, pp 1637-1644, 2006
[7] E.I. Céspedes, C.L. de Korte and A.F.W. Van der Steen, "Echo decorrelation from displacement gradients in elasticity and velocity estimation," IEEE Trans. Ultras., Ferro., Freq. Contr., vol. 46, pp. 791-801, 1999.
[8] W. Aoudi, H. Liebgott, A. Needles, V. Yang, F.S. Foster and D. Vray, "Estimation methods for flow imaging with high frequency ultrasound," Ultrason., vol. 44, pp. 135-140, 2006.
[9] A. Marion, A. Needles and D. Vray, "Blood velocity estimation based on 3D spatiotemporal filtering of sequences of ultrasound images," Proc. of IEEE Ultras. Symp., vol. 1, pp. 2461-2464, 2007.
[10] A. Marion and D. Vray, "Velocity estimation with 3D spatiotemporal filtering of sequences of ultrasound images: a Fourier approach," Proc. of EUSIPCO, 2008.
[11] N. Oddershede, L. Lovstakken, H. Torp and J.A. Jensen, "Estimating 2D vector velocities using multidimensional spectrum analysis, " IEEE Trans. Ultras., Ferro., Freq. Contr., vol. 55, pp. 1744-1754, 2008
[12] J. Meunier and M. Bertrand, "Echographic image mean gray level changes with tissue dynamics: a system-based model study," Trans. Med. Ima., vol. 42, pp. 403-410, 1995.
[13] K.V. Ramnarine, D.K. Nassiri, P.R. Hoskins and J. Lubbers, "Validation of a new blood-mimicking fluid for use in Doppler flow test objects," Ultras. Med. Bio., vol. 24, pp. 451-459, 1998.